

CEBAF Program Advisory Committee Nine Extension and Update Cover Sheet

This update must be received by close of business on Thursday, December 1, 1994 at:
CEBAF 15

User Liaison Office, Mail Stop 12 B
12000 Jefferson Avenue
Newport News, VA 23606

Experiment: **Check Applicable Boxes:**

E_{PR94} - 002



Extension



^{Upgrade}
Update



Hall B Update

Contact Person

Name: Barry M. Freedom
Institution: University of South Carolina
Address: Department of Physics and Astronomy
Address: University of South Carolina
City, State ZIP/Country: Columbia, SC 29208
Phone: (803) 777-6559 **FAX:** (803) 777-2605
E-Mail → Internet: freedom@nuc003.psc.scarolina.edu

CEBAF Use Only

Receipt Date: 12/15/94

By: JP PR 94-132

BEAM REQUIREMENTS LIST

CEBAF Proposal No.: _____

Date: 14Dec94

(For CEBAF User Liaison Office use only.)

List all combinations of anticipated targets and beam conditions required to execute the experiment. (This list will form the primary basis for the Radiation Safety Assessment Document (RSAD) calculations that must be performed for each experiment.)

[illegible]

beam energies, E_{Beam} , available are: $E_{\text{Beam}} = N \times E_{\text{Linac}}$ where $N = 1, 2, 3, 4$, or 5 . For 1995, $E_{\text{Linac}} = 800$ MeV, i.e., available E_{Beam} are 800, 1600, 2400, 3200, and 4000 MeV. Starting in 1996, in an evolutionary way (and not necessarily in the order given) the following additional values of E_{Linac} will become available: $E_{\text{Linac}} = 400, 500, 600, 700, 900, 1000, 1100$, and 1200 MeV. The sequence and timing of the available resultant energies, E_{Beam} , will be determined by physics priorities and technical capabilities.

HAZARD IDENTIFICATION CHECKLIST

CEBAF Proposal No.: _____
(For CEBAF User Liaison Office use only.)

Date: 14Dec94

Check all items for which there is an anticipated need.

Cryogenics <input type="checkbox"/> beamline magnets <input type="checkbox"/> analysis magnets <input checked="" type="checkbox"/> target D_2 type: <u>Ha11 B standard</u> flow rate: _____ capacity: _____	Electrical Equipment <input type="checkbox"/> cryo/electrical devices <input type="checkbox"/> capacitor banks <input type="checkbox"/> high voltage <input type="checkbox"/> exposed equipment	Radioactive/Hazardous Materials List any radioactive or hazadorous/toxic materials planned for use: _____ _____ _____
Pressure Vessels <input type="checkbox"/> inside diameter <input type="checkbox"/> operating pressure <input type="checkbox"/> window material <input type="checkbox"/> window thickness	Flammable Gas or Liquids type: _____ flow rate: _____ capacity: _____ Drift Chambers type: _____ flow rate: _____ capacity: _____	Other Target Materials <input type="checkbox"/> Beryllium (Be) <input type="checkbox"/> Lithium (Li) <input type="checkbox"/> Mercury (Hg) <input checked="" type="checkbox"/> Lead (Pb) <input type="checkbox"/> Tungsten (W) <input type="checkbox"/> Uranium (U) <input type="checkbox"/> Other (list below) <u>carbon</u> <u>iron</u>
Vacuum Vessels <input type="checkbox"/> inside diameter <input type="checkbox"/> operating pressure <input type="checkbox"/> window material <input type="checkbox"/> window thickness	Radioactive Sources <input type="checkbox"/> permanent installation <input type="checkbox"/> temporary use type: _____ strength: _____	Large Mech. Structure/System <input type="checkbox"/> lifting devices <input type="checkbox"/> motion controllers <input type="checkbox"/> scaffolding or <input type="checkbox"/> elevated platforms
Lasers type: _____ wattage: _____ class: _____ Installation: <input type="checkbox"/> permanent <input type="checkbox"/> temporary Use: <input type="checkbox"/> calibration <input type="checkbox"/> alignment	Hazardous Materials <input type="checkbox"/> cyanide plating materials <input type="checkbox"/> scintillation oil (from) <input type="checkbox"/> PCBs <input type="checkbox"/> methane <input type="checkbox"/> TMAE <input type="checkbox"/> TEA <input type="checkbox"/> photographic developers <input type="checkbox"/> other (list below) _____ _____	General: Experiment Class: <input checked="" type="checkbox"/> Base Equipment <input type="checkbox"/> Temp. Mod. to Base Equip. <input type="checkbox"/> Permanent Mod. to Base Equipment <input type="checkbox"/> Major New Apparatus Other: _____ _____

Photoproduction of Vector Mesons off Nuclei

Spokespersons: P.-Y. Bertin, M. Kossov, and B.M. Preedom

W. Brooks, V. Burkert, D. Joyce, B. Mecking, M.D. Mestayer,
B. Niczyporuk, E.S. Smith, R.R. Whitney, A. Yegneswaran
CEBAF, Newport News, Virginia

D.C. Doughty, D.P. Heddle, M.V. Kossov, Z. Li
Christopher Newport University, Newport News, Virginia

S. Boiarinov, P. Degtyarenko, E. Doroshkevich,
N. Pivnyuk, O. Pogorelko, A. Vlassov
Institute of Theoretical and Experimental Physics, Moscow, Russia

C. Hyde-Wright, A. Klein, S. Kuhn, L. Weinstein
Old Dominion University, Norfolk, Virginia

L. Elouadrhiri, R.S. Hicks, R. Miskimen, G.A. Peterson, K. Wang
University of Massachusetts, Amherst, Massachusetts

A. Coleman, M. Eckhause, H. Funsten,
J. Kane, P. Rubin, T. Tung, R. Welsh
College of William and Mary, Williamsburg, Virginia

L. Dennis and P. Dragovitsch
Florida State University, Tallahassee, Florida

M. Gai
Yale University, New Haven

G.S. Blanpied, C. Djalali, B.M. Preedom, C.S. Whisnant
University of South Carolina, Columbia, SC 29208

P.-Y. Bertin
Université Blaise Pascal, F63177, Aubière CEDEX, France

G. Audit, P.A.M. Guichon, M. Guidal,
J. Marroncle, L.Y. Murphy, B. Saghai
Centre d'Etudes de Saclay, F91191, Gif-sur-Yvette CEDEX, France

OVERVIEW

This proposal is based on ideas presented in two earlier letters of intent: LOI-89-01 by P.-Y. Bertin and P.A.M. Guichon, and LOI-93-004 by B.M. Freedom and P.Y. Bertin. The proposal aims at determining the properties of vector mesons in nuclear matter. At high baryon density the mass of vector mesons is predicted to change due to chiral symmetry restoration. The predicted downward shift of the vector meson mass is 10 % or about 100 MeV. The photoproduction of vector mesons near threshold can be used to measure the mass of vector mesons embedded in nuclear matter. At CEBAF energies, the production of ρ -mesons off heavy nuclei is the ideal experiment to determine the ρ -meson mass shift in nuclear matter. A second possibility is to measure the mass shift for narrow vector mesons. Because of the long decay length $c\tau$, only a small fraction of these vector mesons will decay inside the nucleus. However, since the mass shift is predicted to be substantial relative to the natural width, these decays will be easier to separate from vector mesons decaying outside of the nucleus.

Detecting the leptonic decays of vector mesons is the only reliable way to measure the mass shift of vector mesons, because the hadronic decay in nuclear matter is always disturbed by final state interactions. The small cross sections of incident photons and outgoing electrons for secondary interactions with nuclear matter makes this reaction the ideal probe for testing the properties of the dense central region of the nucleus without significant input and output distortions. We propose to measure the $A(\gamma, e^+e^-)A'$ reaction, which can be identified in the CLAS detector. Energy deposition in the electromagnetic calorimeter, Cerenkov counter signal, and transverse momentum compensation define clear cuts for the separation of the e^+e^- events from the large hadronic background.

We propose to take data on four nuclear targets simultaneously: deuterium, carbon, iron, and lead with a beam intensity of $5 \cdot 10^7$ tagged photons per second in the energy range $1.2 \div 2.2$ GeV ($E_0 = 2.4$ GeV). Setting the magnetic field of the CLAS detector to half its maximum value was found to be optimal for this photon energy range. Tagged photons are used to determine kinematics of the reaction. In the off-line analysis, the e^+e^- mass spectra can be analysed under different kinematical conditions. Specifically, coherent vector meson production, which is expected to take place outside of the nucleus, can be suppressed by detecting the recoiling nucleon (proton or neutron).

1. Introduction.

Vector mesons play an important role in photonuclear reactions because they carry the same quantum numbers as the incident photon. It has recently been suggested by G.E. Brown and M. Rho [1] that the mass of vector mesons could decrease with increasing baryon density. This phenomenon would provide a physical observable for chiral symmetry (χ^S) restoration at high baryon density, an essential non-perturbative phenomenon associated with the structure of quantum chromodynamics (QCD). According to the constituent quark model the difference between the mass of the valence quark (m_v) and the mass of the current quark (m_c) is expected to be proportional to the mean vacuum value of the quark condensate: $m_v - m_c \propto \langle \psi\psi \rangle_v$. The mass difference appears because of chiral symmetry breaking (χ^{SB}). QCD sum rule calculations [2] show that the value of this difference is about 300 MeV for all quarks. If the mean vacuum value differs from that for the hadron density in nuclei, then the constituent quark mass should be renormalized as follows: $m'_v = m_c + \frac{\langle \psi\psi \rangle_n}{\langle \psi\psi \rangle_v} \cdot 300 \text{ MeV}$, where the indices n correspond to nuclear matter and v to vacuum. The same conclusion was reached in a nuclear matter model based on quark degrees of freedom [3,4]. Using the symmetry properties of QCD in an effective Lagrangian theory, Brown and Rho [1] have found a scaling law for the vector meson masses at finite baryon density: $\frac{M_N^n}{M_N^v} = \frac{M_V^n}{M_V^v} = \frac{f_\pi^n}{f_\pi^v}$, where f_π is the $\pi \rightarrow \mu\nu$ decay constant playing the role of an order parameter for the chiral symmetry restoration. At nuclear density the value of f_π was found to be 15-20% smaller than in vacuum. In contrast to the constituent quark model, it was found that $\frac{M^n}{M} = (\frac{\langle q\bar{q} \rangle_n}{\langle q\bar{q} \rangle_v})^{1/3}$.

The dependence of the density of the quark condensate on the nuclear density [5] is shown in Fig. 1(a,b) for two values of the nucleon σ term: $\sigma_N = 30 \text{ MeV}$ and $\sigma_N = 45 \text{ MeV}$. The solid lines are for the Nambu–Jona-Lasinio chiral quark-meson model [6], the dashed lines are for the Gell-Mann–Levy chiral quark-meson model [7]. Nevertheless, the issue of the mean value of the quark condensate in nuclear matter is not completely resolved from the theoretical point of view. According to a recent estimate [8] the mean value of the quark condensate in nuclear matter first decreases with increasing nuclear density, then rises and, at mean nuclear density, becomes 5% larger than in vacuum (Fig. 1(c)). This is presently the only calculation which does not predict a significant shift for the vector meson masses. The mean value of the theoretical predictions for the mass shift for vector mesons is about 100 MeV.

The characteristic features of the vector mesons are shown in Table 1. In addition to the well known lepton and hadron branching ratios, the table contains the vector meson masses and widths and the masses of the first excited vector meson state (V') which determine the coherence length l_c . Even at 2 GeV the boosted coherence length (the tabulated value should be multiplied by the γ factor E_γ/m_V) is of the order of 1 fm, only. It is small enough to be neglected in comparison to the

a) True coincident e^+e^- background results from Bethe-Heitler pairs, from Dalitz decay of a π^0 or η , and from coincident multiple π^0 production where each Dalitz decays. The Bethe-Heitler pairs can be removed by using the measurement of t to exclude coherent events. Electron pairs from Dalitz decay have an invariant mass below the mass of the π^0 or η . The background from coincident Dalitz decays can be measured by detecting like-sign electrons.

b) Random coincident e^+e^- background results from Compton scattering from atomic electrons followed by Bethe-Heitler production from the scattered photon. If the Bethe-Heitler production occurs in a target downstream from the Compton scattering, the vertex reconstruction will reject it. If not, then an e^-e^- measurement will determine the contribution where the Compton scattered electron is detected while a missing mass calculation on e^+e^- pairs will exclude subsequent Bethe-Heitler production.

c) Misidentified π^+ and/or π^- were discussed in the proposal. The suppression factor for a single pion is $\sim 10^{-4}$ and for coincident pions is $\sim 10^{-8}$.

Effect of multiple targets on the background:

The primary adverse effect due to the multiple targets is the bremsstrahlung of one or both of the pair electrons as discussed in the proposal. To minimize this effect, both the Fe target (7% radiation length) and the Pb target (16% radiation length) will be multiple targets each having 6 equal segments separated by 0.5 cm to reduce the amount of matter seen by an exiting electron. Aside from the bremsstrahlung of the pair electrons, there will be a reduction in the photon flux due to the accumulating target thickness but the photons remaining in the beam will still retain their tagged energy.

Sensitivity to a vector meson mass reduction:

As presented in the proposal, the mass resolution of CLAS is approximately 4 MeV at an invariant mass of 750 MeV and 6 MeV at 1 GeV. These resolutions are comparable to or less than the intrinsic widths of the vector mesons and significantly less than the predicted shifts in the vector meson masses. In order to visualize a measurable effect of a shift in the mass, we have made the calculations presented in fig. 3 for shifts of $\Delta M = 0, 40 \text{ MeV}, 100 \text{ MeV}$ and for comparison -40 MeV . The figure shows the ratio of the invariant mass spectrum calculated for Pb to that calculated for deuterium. The calculations sum up the results for all gamma energies between 1.2 and 2.2 GeV but use the tagged energy information to take account of the effective mass number (A_{eff}) energy dependence predicted by the vector dominance model. No density dependent change in the widths or the relative phases of the vector mesons was used. The width of the ρ uses the prescription of Jackson (Nuovo Cimento **34**, 1644 (1964)).

Update of Proposal PR-94-002

Photoproduction of Vector Mesons Off Nuclei

Spokespersons: P.-Y. Bertin, M. Kossov, B.M. Freedom

PAC8 deferred this proposal with the following comments:

PAC likes the motivation for this measurement and believes that an unambiguous demonstration of a reduction in the vector meson mass would be an important result. However, the proposed experiment is not convincing and the projected sensitivity marginal. PAC was not convinced that the detector acceptance, the background and the effect of multiple targets on the background were optimal for the proposed measurement. PAC urges the proposers to work on developing an experiment which can provide a significantly increased sensitivity to a vector mass (sic) reduction. This sensitivity should be quantified in terms of the uncertainty in the appropriate experimental observables.

The following information addresses these comments. It is assumed that PAC9 has copies of the proposal which we attach to this update.

Detector Acceptance:

Aside from the ω and ϕ acceptances shown in the proposal, we have calculated the invariant mass distributions with and without the CLAS acceptance in figures 1 and 2 for deuterium and Pb at gamma energies of 1.4, 1.8, and 2.2 GeV. The energy dependence is primarily due to the opening angles associated with the center of mass motion of the decaying particle. While this effect is significant at 1.4 GeV for all three vector mesons and at 1.8 GeV for the ϕ , the actual momentum dependence of the acceptance of the CLAS detector will need to be well known for all CLAS experiments including this experiment.

Background:

Because we will use a tagged beam, most of the possible backgrounds can be eliminated. Using the measured t allows for the separation of coherent processes from incoherent production. Missing mass can be calculated knowing the detected invariant mass. Events having a total energy greater than the tagged energy can be excluded. Also since the experimental trigger is coincident e^+e^- pairs, the start counter is not necessary and the mini-toroid can be used to remove the low energy electrons produced by Compton scattering in the targets.

The background is of three types: a) true coincident e^+e^- , b) random coincident e^+e^- , and c) misidentified π^+ and/or π^- .

LAB RESOURCES REQUIREMENTS LIST

CEBAF Proposal No.: _____
(For CEBAF User Liaison Office use only.)

Date: 14Dec94

List below significant resources — both equipment and human — that you are requesting *from CEBAF* in support of mounting and executing the proposed experiment. Do not include items that will be routinely supplied to all running experiments, such as the base equipment for the hall and technical support for routine operation, installation, and maintenance.

Major Installations	(either your equip. or new equip. requested from CEBAF)	Major Equipment
----------------------------	--	------------------------

Magnets

Power Supplies

Targets

Detectors

Electronics

Computer Hardware

Other

Other

standard Hall B resources

Data Acquisition/Reduction

Computing Resources: _____

New Software: _____

deuterium no fermi momentum $\rho, \omega, \phi, \rho\omega$ and $\rho\phi$

$N(M_{\pi\pi})/\gamma$ $0.10 < -t < 9.99 \text{ GeV}^2$ $A_{\text{eff}} = \text{VDM}$ $\Delta M = -.000 \text{ GeV}$

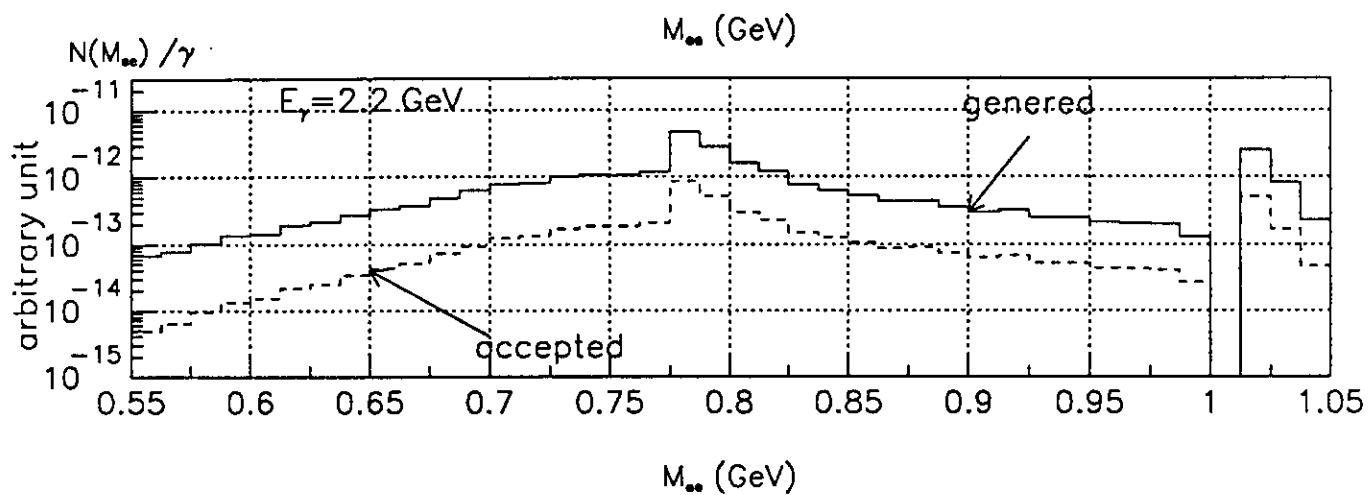
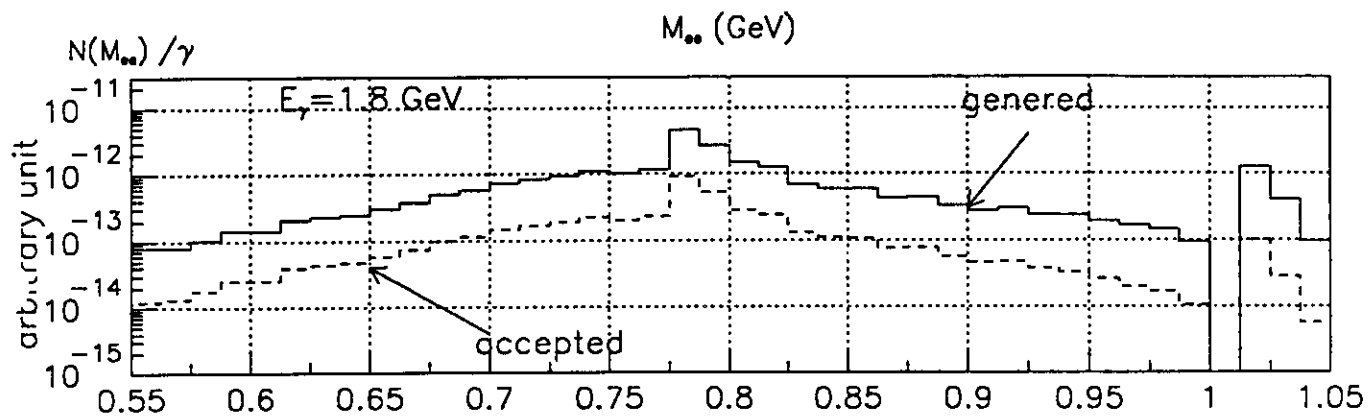
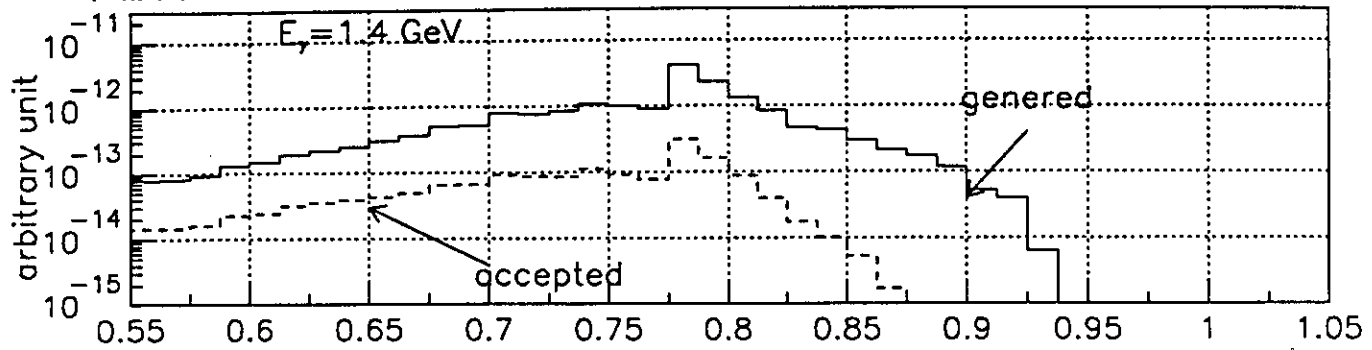


Figure 1

The calculations restrict $-t$ to be greater than 0.1 GeV^2 to avoid the region of coherent production. The events were generated assuming incoherent photoproduction in the vector dominance model with Pauli blocking and a Fermi momentum of $200 \text{ MeV}/c$ for Pb. The $\rho\omega$ and $\rho\phi$ interferences are included. The shift in mass follows the prescription of Guichon and Bertin -- see references 3 and 4 of the proposal. The calculations include the acceptance of CLAS. The most apparent effect occurs for the ρ since most of the ω and the ϕ decays occur outside of the nucleus due to their longer lifetimes.

Quantification of the sensitivity:

In fig. 4 we present the sensitivity to the mass shift using the reduced χ^2 to yield a confidence level. The χ^2 is calculated for the ratio of Pb to deuterium. The expected value for the ratio is taken to be unity so that this reduced χ^2 is a measure of the goodness of the assumption of unity. The figure shows that we can observe a mass shift as small as 20 MeV with a confidence level better than 90% .

lead with fermi momentum = 200 MeV/c $\rho, \omega, \phi, \rho\omega$

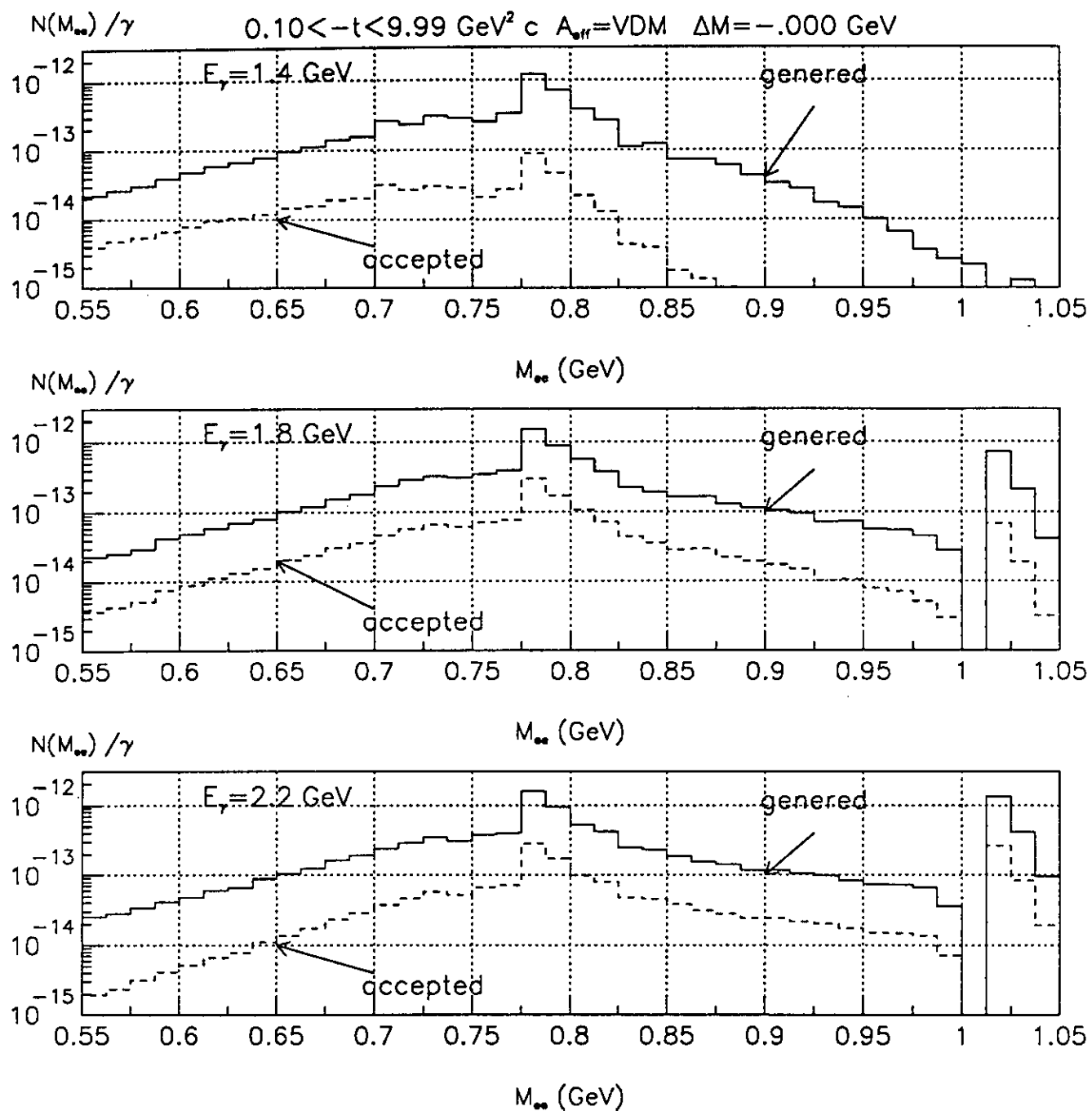


Figure 2

nuclear radius. The formation length l_f , a parameter of the Vector Meson Dominance (VMD) model, which determines the photon absorption in nuclear matter is shorter by a factor of two. Therefore, we do not expect any significant distortion due to shadowing. The main parameters of the table are the decay length ($c\tau$) and the cross section for vector meson interaction with nuclear matter. We expect the maximum count rate at $E_\gamma = 1.5$ GeV where both ρ and ω production cross sections reach their maximum values (Fig. 2). For this energy all length scales are boosted by a factor of two. Thus, the decay length is expected to be 2.5 fm for the ρ -meson, 45 fm for the ω -meson, and 85 fm for the ϕ -meson. These lengths should be compared to the radii of the target nuclei: 2.5 fm for carbon, 4.5 fm for iron, and 6.5 fm for lead. A simple calculation shows that 63% of the ρ -mesons will decay inside carbon, 83% inside iron, and 93% inside lead. For the narrow vector mesons the situation is different: even inside lead, only 13% of the ω -mesons and 7% of the ϕ -mesons will decay. However, the shifted e^+e^- mass distribution for the narrow vector mesons should be clearly separated from that for the vacuum decay. It should be mentioned that according to Bertin and Guichon [3] the ϕ -meson is not expected to be shifted because in first approximation the ϕ does not couple to the nuclear field.

Table 1. Characteristics of the Vector Mesons.

Parameter	ρ -meson	ω -meson	ϕ -meson
Lepton branching (Γ_l/Γ)	e^+e^- (0.0044%)	e^+e^- (0.0072%)	e^+e^- (0.031%)
Hadron branching (Γ_h/Γ)	2π (100%)	3π (89%), 2π (2%)	$2K$ (84%), 3π (12%)
m_V (MeV)	768.	782.	1019.
Γ_V (MeV)	151.5	8.4	4.4
$m_{V'}$ (MeV)	1465.	1394.	1680.
$c\tau$ (fm)	1.3	23.4	44.4
σ_{VN} (mb)	21.	21.	12.
$l_f = 1/\Delta m_V$ (fm)	0.26	0.26	0.23
$l_c = 2/m_V$ (fm)	0.52	0.51	0.39

The diagrams for vector meson photoproduction off nuclei are shown in Fig. 3. The production mechanisms were discussed in detail in the proposal PR-93-012 "Electroproduction of Light Quark Mesons" for hydrogen and deuterium targets. It was shown that the diffractive mechanism (Fig. 3a) and One Pion Exchange (OPE) mechanism (Fig. 3b) give the bulk of the vector meson production. ρ -meson production is dominated by the diffractive mechanism. The OPE mechanism can be isolated by subtracting the diffractive contribution from the ω -meson production which is approximately equal to one ninth of the diffractive contribution to the ρ -meson production. Isolation of the OPE contribution will allow the investigation of the pionic degrees of freedom in nuclear matter.

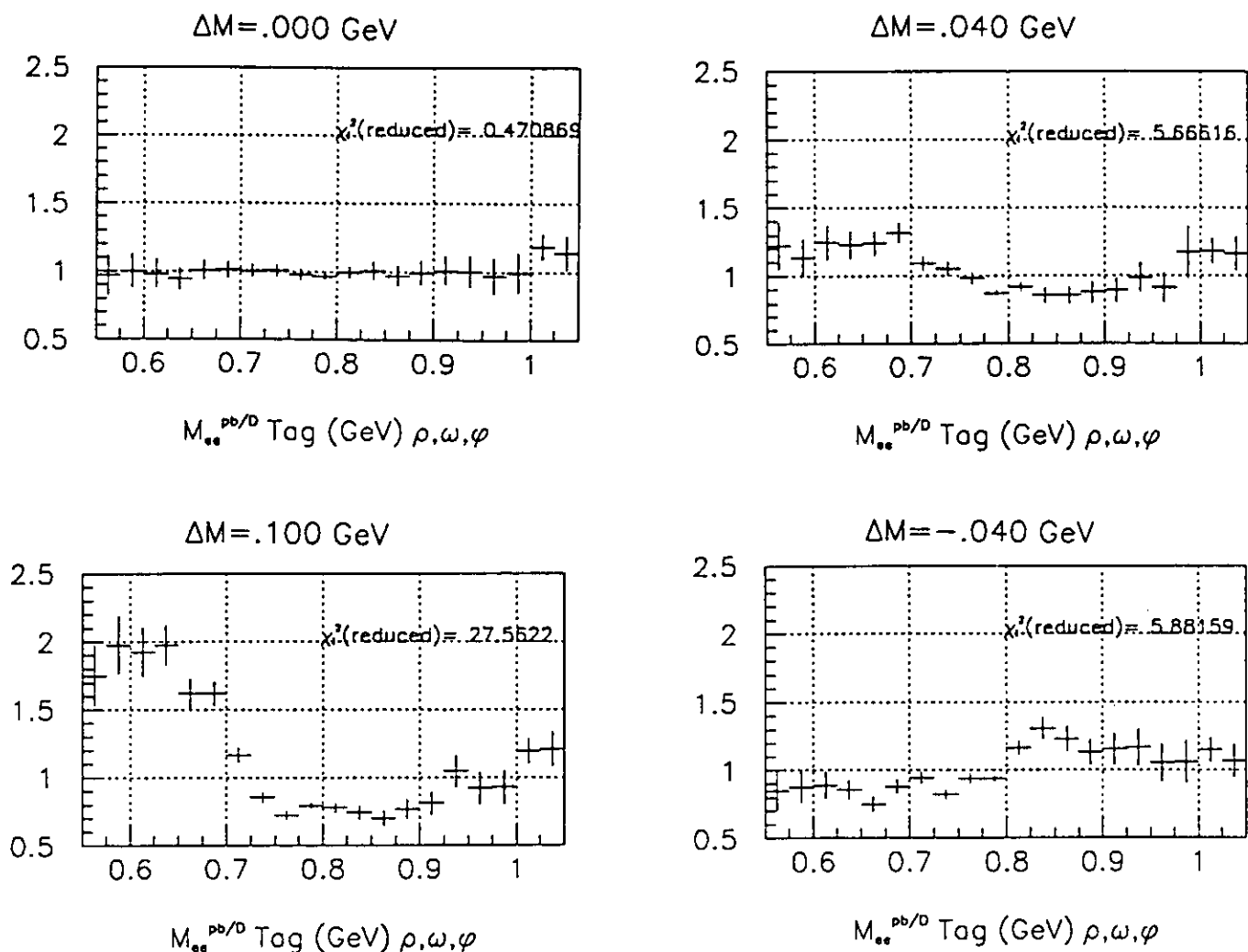


Figure 3

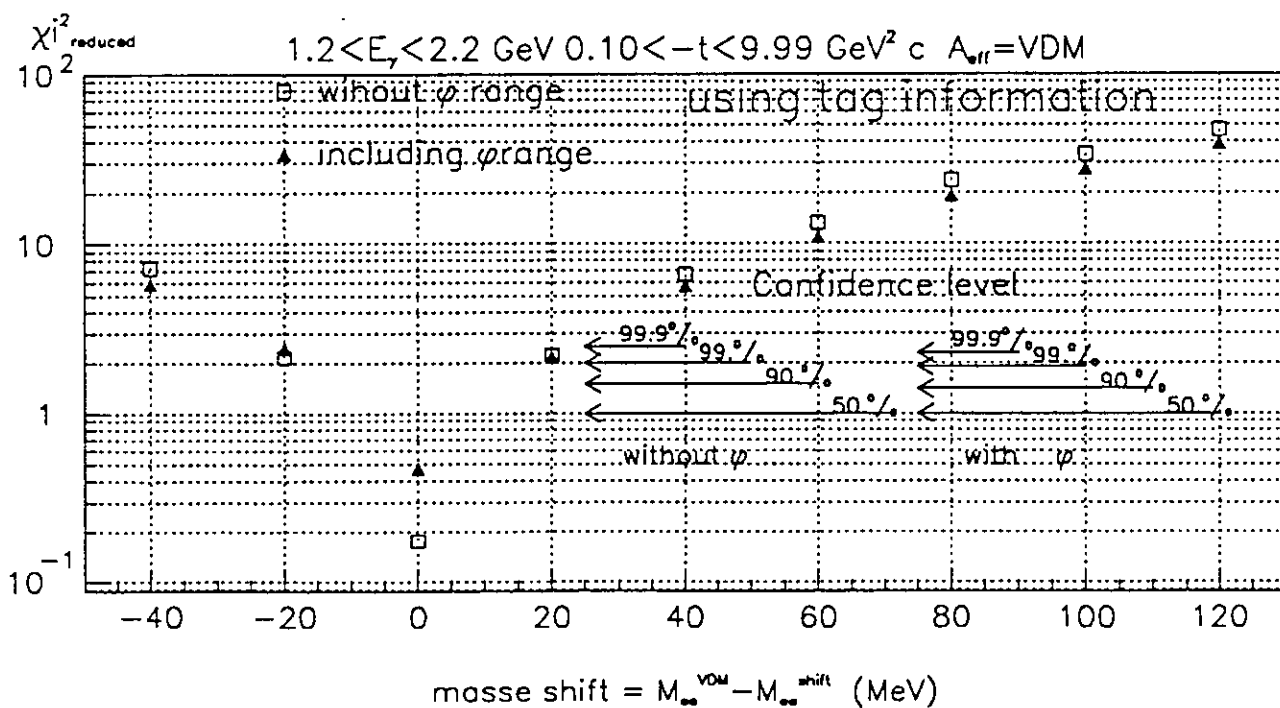


Figure 4

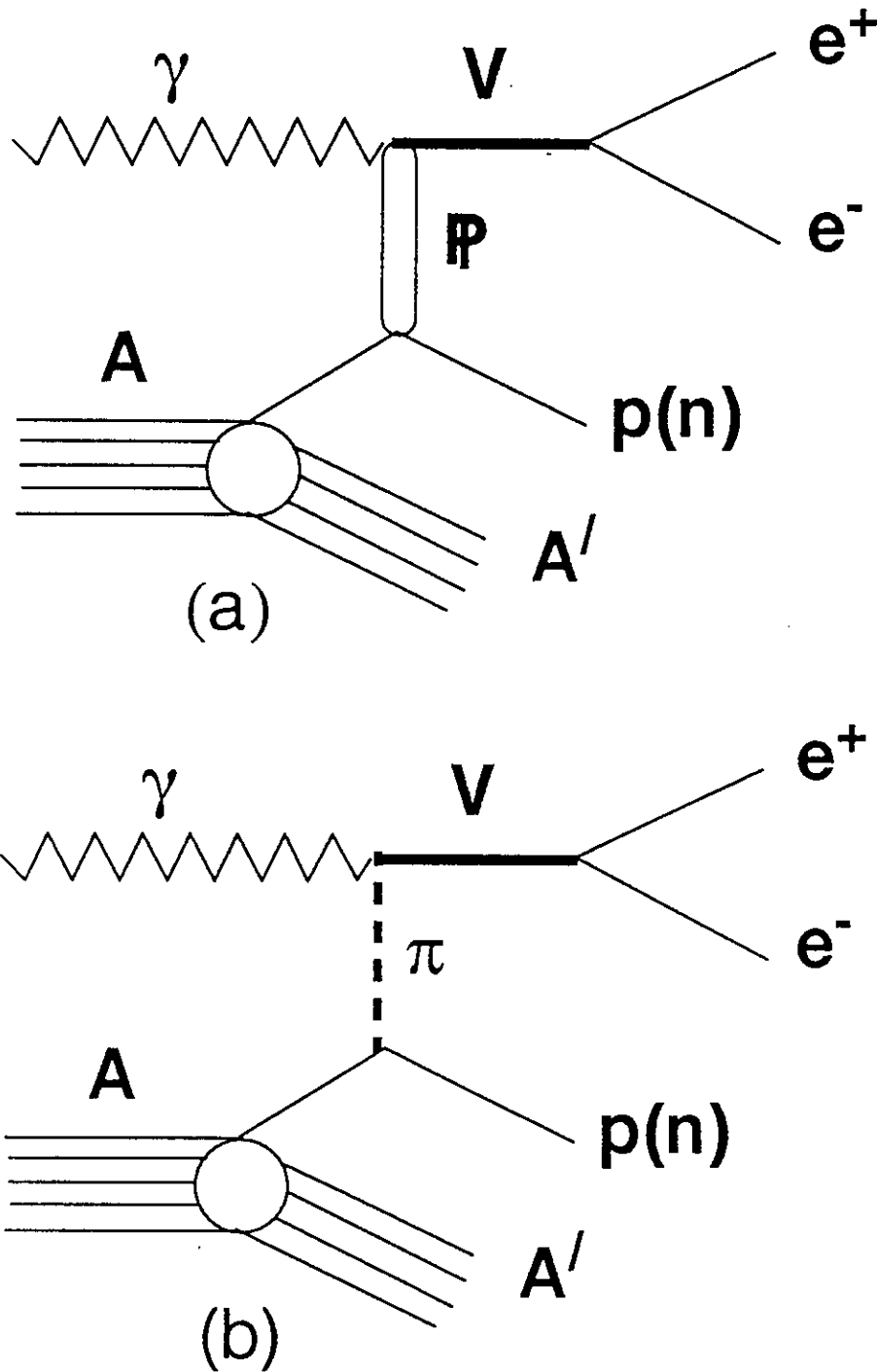


Fig.3. Feynman diagrams of Vector Meson Photoproduction off nuclei.
 a. Diffractive photoproduction of Vector Mesons;
 b. One Pion Exchange mechanism of photoproduction.

To measure the mass shift in nuclear matter for vector mesons the following conditions should be fulfilled:

- (i) Photoproduction off heavy nuclei to increase the probability for the vector meson to decay inside the nucleus.
- (ii) Photoproduction near threshold to keep the boost small.
- (iii) Option to utilize detection of the recoiling nucleon to suppress coherent production.

The first rough simulation was made without taking the ρ/ω mixing into account [3]. The results of the simulation for heavy nuclei are shown in Fig. 4. One can clearly see the shift of the ρ -meson mass. More complicated calculations taking the ρ/ω mixing into account [9] are shown in Fig. 5 for different ρ mass shifts. The ρ/ω mixing effect emphasizes the effect of the mass shift in the region to the left of the sharp ω -meson peak. The attractive feature of the proposed measurements is the direct comparison of a vector meson that decays mostly inside the nucleus (ρ -meson) with a vector meson that decays mostly outside of the nucleus (ω -meson).

2. Existing Data.

2.1. K^+ -nucleus scattering and the vector meson mass shift.

Elastic and total cross sections for K^+ -nucleus scattering are sensitive to the density-dependent effective masses of the vector mesons whose exchange is thought to be responsible for the dominant part of the low energy K^+ -nucleon interaction, since one-pion exchange is not allowed [10]. In this respect, the K^+ interacts with a nucleon the same way as a virtual photon. In Fig. 6 one can see the sensitivity of the measurements [11]. The λ parameter denotes the percentage of the vector meson mass reduction. The best fit to the data corresponds to a 10% mass reduction.

2.2. Photoproduction of vector mesons off nuclei.

Vector meson properties in nuclear matter were discussed by Friman and Soyeur [9] on the basis of the existing experimental data [12,13]. It was pointed out that, at present, there are no data on the electromagnetic production of vector mesons off nuclei at low energies (near threshold). On the other hand, the existing data at $\nu = 3 \div 5$ GeV correspond to light nuclear targets (Be and C). As a result, only a small fraction of the ρ -mesons can decay inside the nucleus. Therefore, the existing experiments are not sensitive to the mass shift.

The contribution of the Bethe-Heitler (BH) process which increases with the atomic number of the nucleus as Z^2 has to be subtracted from the measured (e^+e^-) mass distribution (Fig. 7, [14]). This can be an additional source of systematic errors for vector meson photoproduction off heavy nuclei. It should be noted that the detection of the secondary nucleon will eliminate the contribution of the Bethe-Heitler process.

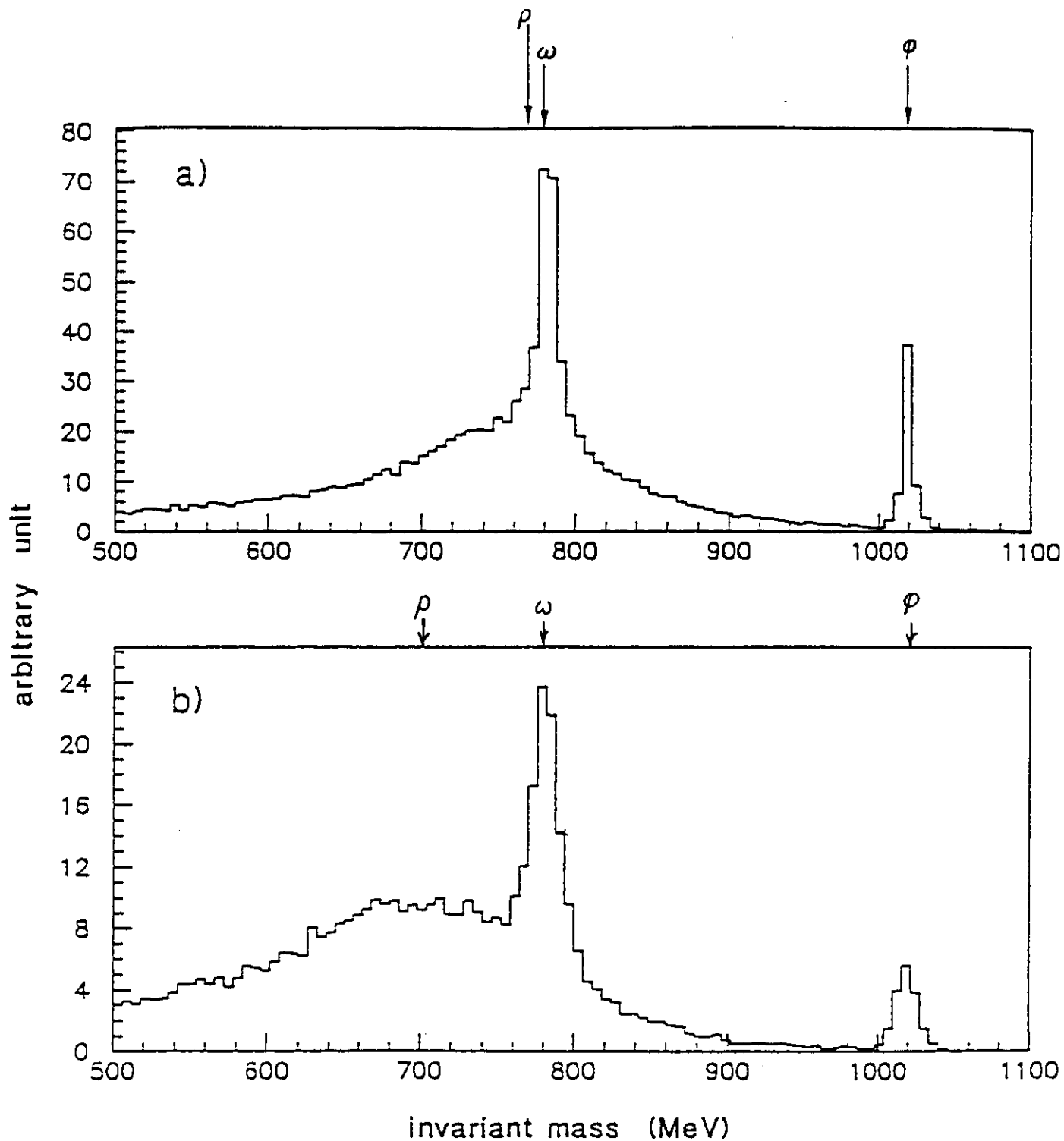


FIG. 4. Number of (e^+e^-) pair vs their invariant mass in arbitrary units: (a) No nuclear effects are included. (b) Full calculation with cut of five degrees as explained in the text.

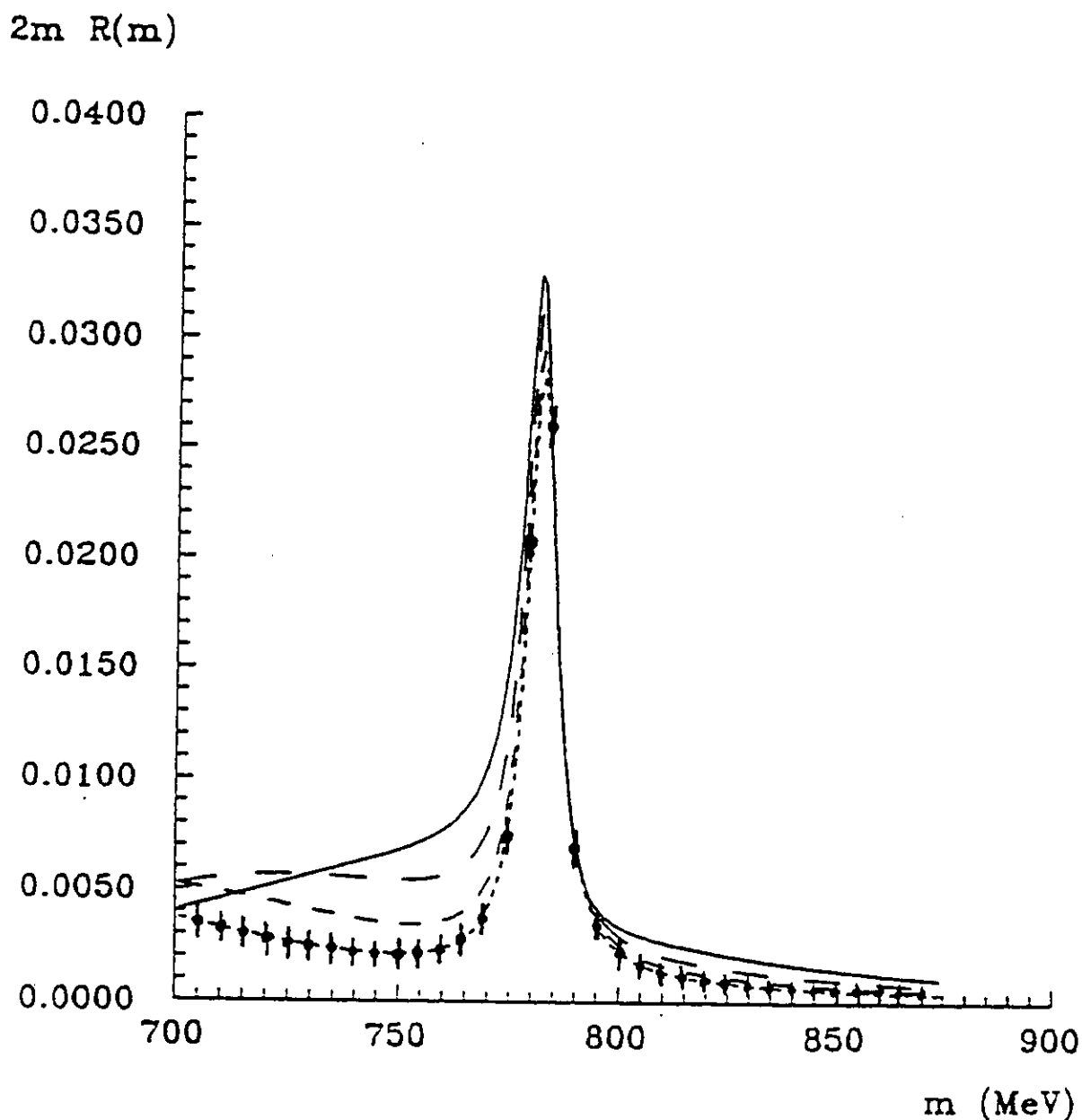


Figure 5.
 (e^+e^-) invariant mass spectrum associated to diffractive processes $\gamma \rightarrow V \rightarrow e^+e^-$ in the $Be(\gamma, e^+e^-)$ reaction analyzed with different values of the ρ -meson mass : 768 MeV (solid line), 738 MeV (long-dashed line), 708 MeV (intermediate dashed line), 678 MeV (short-dashed line).

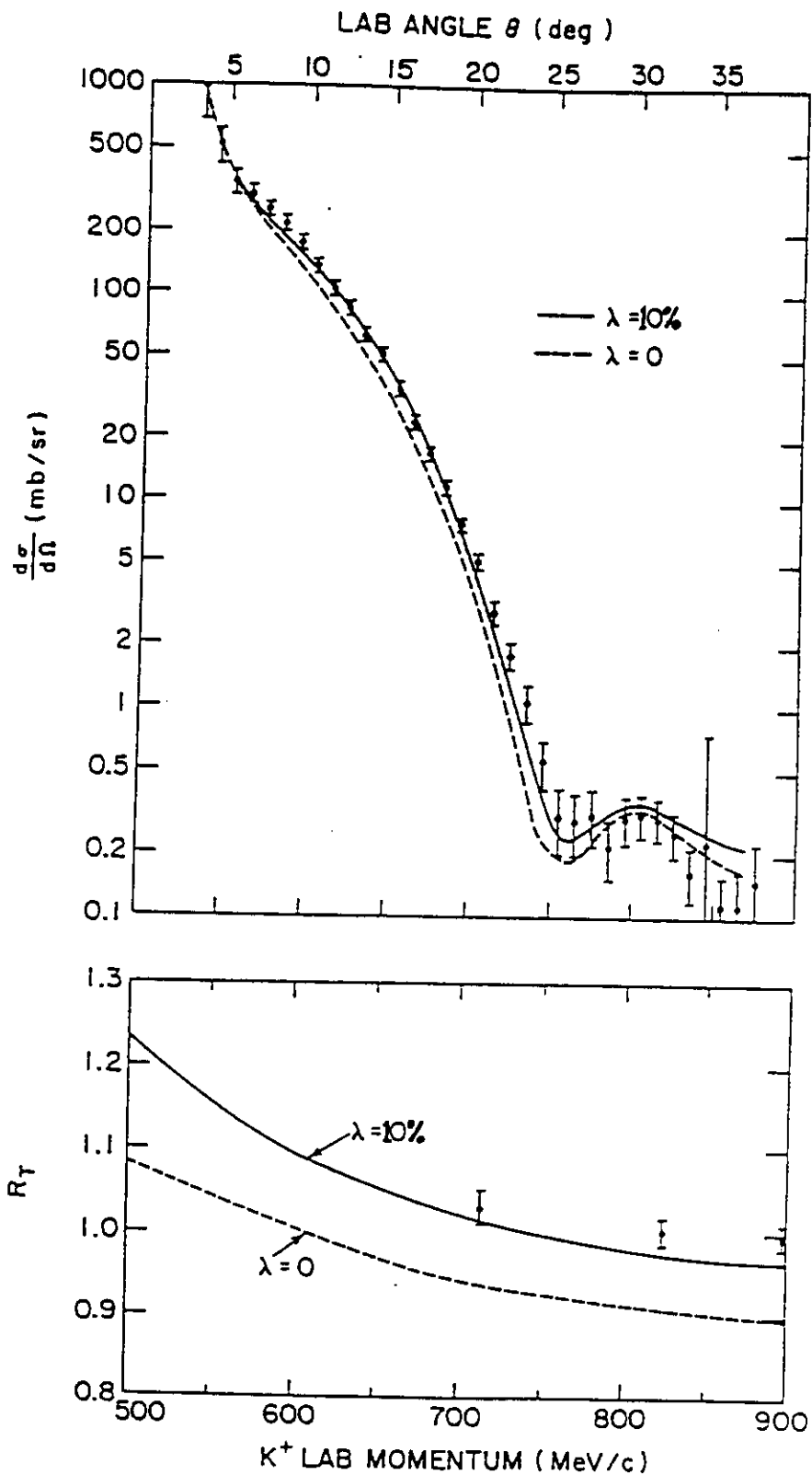


FIG. 6. The angular distribution for $K^+ + {}^{12}\text{C}$ elastic scattering at 800 MeV/c is shown at the top. At the bottom is shown the total cross-section ratio $R_T = \sigma_{\text{tot}}(K^+ + {}^{12}\text{C}) / 6\sigma_{\text{tot}}(K^+ + d)$.

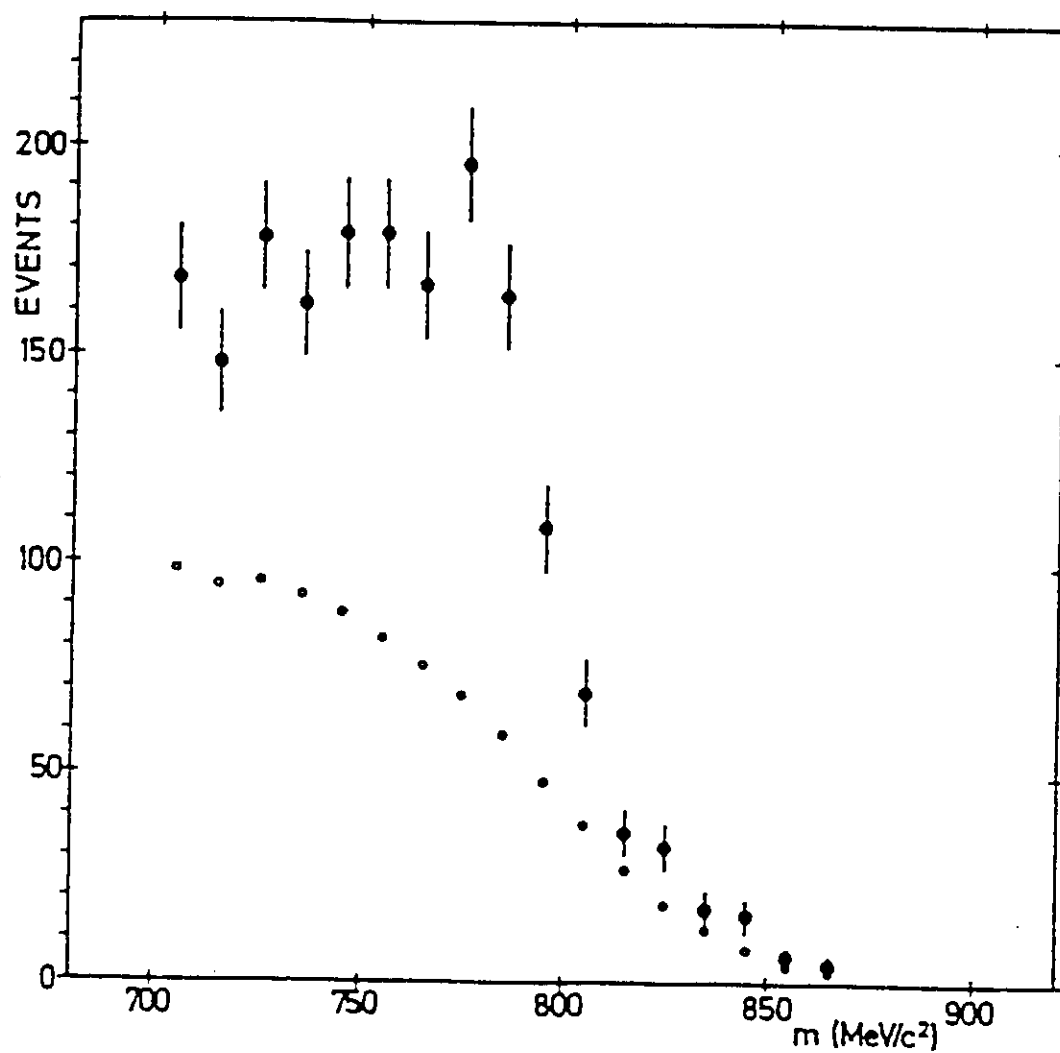


Fig. 7. The black dots are the experimentally measured event distribution. The open circles are the calculated contribution of the BH process.

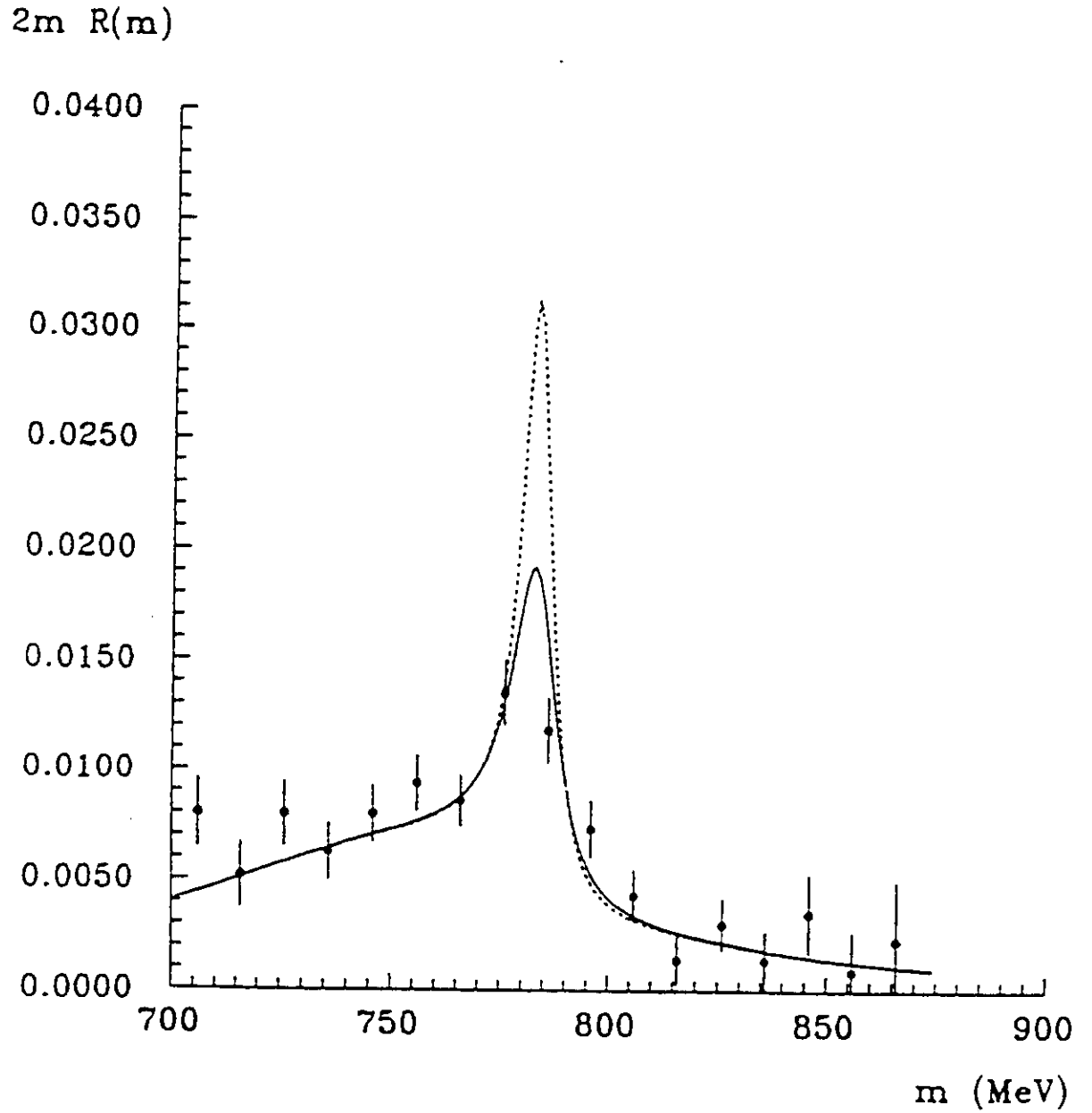


Figure 8.
 (e^+e^-) invariant mass spectrum associated to diffractive processes $\gamma \rightarrow V \rightarrow e^+e^-$ in the
 $Be(\gamma, e^+e^-)$ reaction at $E_\gamma = 5.1$ GeV. The data and the solid curve are from Ref.
 [14]. The dotted line is the result of an analysis made with updated parameters (m, Γ) [9].

In Fig. 8 the subtracted (e^+e^-) invariant mass spectrum is shown. The dotted line was calculated for the free values of the vector meson parameters. At high energy ($E_\gamma = 5.1$ GeV) and on a light nucleus, the existing experimental data can be described without using a ρ -meson mass shift.

There are no data for ϕ -meson photoproduction off nuclei in the $A(\gamma, e^+e^-)$ reaction. It has been predicted that the reduction in the ϕ -meson mass is dependent on the amount of strangeness in the nucleon [15]. In Fig. 9 one can see the predicted mass shift for the ϕ -meson for two values of $y = \frac{2\langle s\bar{s} \rangle_N}{(\langle u\bar{u} \rangle_N + \langle d\bar{d} \rangle_N)}$.

3. Proposed Experiment.

3.1. Experimental Procedure.

The proposed experiment will use the CEBAF Large Acceptance Spectrometer CLAS to measure e^+e^- pairs resulting from vector meson photoproduction off nuclear targets. The main goal of the experiment is to measure the shift of the vector meson mass in nuclear matter. The large acceptance of the CLAS detector will allow to measure the e^+e^- mass spectrum in a wide range of kinematics, ranging from coherent production at small angles to incoherent production at large angles. Particle identification in CLAS allows to separate the leptonic decay of the vector mesons from the large hadronic background. In addition, detection of the recoiling nucleons will make it possible to suppress the Bethe-Heitler background and coherent vector meson production.

The data acquisition system will be triggered by the detection of two electromagnetic particles with opposite charges. A typical ρ photoproduction event at $E_\gamma = 1.5$ GeV is shown in Fig. 10. In the hexagonal insert a longitudinal view of the event is shown. The sector plane (mid plane of each sector) projection represents all six sectors (sectors 1-3 and sectors 2-4 are superimposed). A Monte-Carlo program was used to estimate the detection efficiency of CLAS for e^+e^- events. The efficiency is shown in Fig. 11 as a function of the photon energy E_γ for ω and ϕ -mesons. The efficiency was calculated under the condition that both electron and positron were detected by all 6 drift chambers, by TOF scintillator counters, by Cerenkov counters, and by the electromagnetic calorimeters. The solid curves were calculated with good statistics by a fast Monte-Carlo program that describes the detector geometry approximately. The points in the figure were obtained by a full reconstruction of simulated individual events. The dashed line was calculated under the additional condition that the recoiling proton was detected by drift chambers and scintillation counters.

The π/e rejection in the CLAS detector for particles with 1 GeV/c momentum is sufficient to suppress the large hadronic background from $\pi^+\pi^-$ pairs. Comparing the energy deposition in the electromagnetic calorimeter with the momentum obtained from the trajectory analysis gives a pion suppression by a factor $2 \cdot 10^{-2}$,

the Cerenkov counter signal will suppress pions by a factor $4 \cdot 10^{-3}$. The resulting total suppression factor (10^{-4}) should be compared to the branching ratios: $4 \cdot 10^{-5}$ for ρ -mesons, $7 \cdot 10^{-5}$ for ω -mesons. We will require that both particles are identified as electrons, hence the contamination of the event sample by pion pairs can be estimated to be around 10^{-4} . The $\gamma p \rightarrow n\pi^+\pi^0$ ($\gamma n \rightarrow p\pi^-\pi^0$) reaction and accidental coincidences between electrons (positrons) and hadronic background increase this contamination to the 10^{-3} level. The background of e^+e^- pairs from the $\gamma N \rightarrow N\pi^0\pi^0$ reaction is approximately of the same order and can be removed in the off-line analysis (large missing energy, additional electromagnetic particles in the event).

For heavy nuclei, the effective mass distribution could be distorted by the Coulomb final state interaction of the electrons with the nuclear field. This is an obvious difference between the decay inside and outside of the nucleus. In a crude estimate, we simulated the e^+e^- decay inside the nucleus and added 10 MeV to the e^- and subtracted 10 MeV from the e^+ . The modification of the electron momenta is comparable to the experimental momentum resolution (7 MeV/c). The resulting mass shift is $1 \div 2$ MeV. Our conclusion is that final state interaction of the electrons with the nuclear Coulomb field cannot generate the effect of chiral symmetry restoration in nuclear matter.

3.2. Cross Section Calculation and Count Rate Estimates.

For the description of the cross section for ρ and ω -meson production we used the same model for vector meson production [16-18] that was used in PR-93-012 for the estimation of the vector meson production on a hydrogen target.

The cross section for vector meson production at 1.5 GeV is fairly high (25 μb). For a 1 g/cm² target, $5 \cdot 10^7$ photons per second, and in the 1.2 \div 2.2 GeV tagged photon energy range, 700 ρ -mesons are produced per second. The small branching ratio for the e^+e^- decay reduces this number by a factor $4.4 \cdot 10^{-5}$, i.e. about 20 e^+e^- decays of the ρ -meson can be detected per hour (at 20% detection efficiency). Approximately 10 e^+e^- pairs will be detected as a result of ω decay (the production cross section is 7 μb , i.e. 200 ω -mesons per second). As a result, 30 ρ and ω vector mesons will be detected per hour. According to this estimate, the total event sample for light nuclei (¹²C) will reach 10^4 events in 288 hours. This is an order of magnitude larger than the total world statistics (700 events for the ¹²C target (NINA) + 1200 events for the ⁹Be target (DESY)). In addition to the large event sample, the main advantage of our data is the closeness to the production threshold. For heavy targets our data will be unique. Detection of the secondary nucleon can reduce the Bethe-Heitler contribution, if necessary. The CLAS detector has approximately 60% acceptance for the forward nucleons. Another option to suppress the coherent process for heavy nuclei is eliminate events with small $-t$. It should be noted that near threshold $-t_{min}$ is large, and the coherent contribution is small.

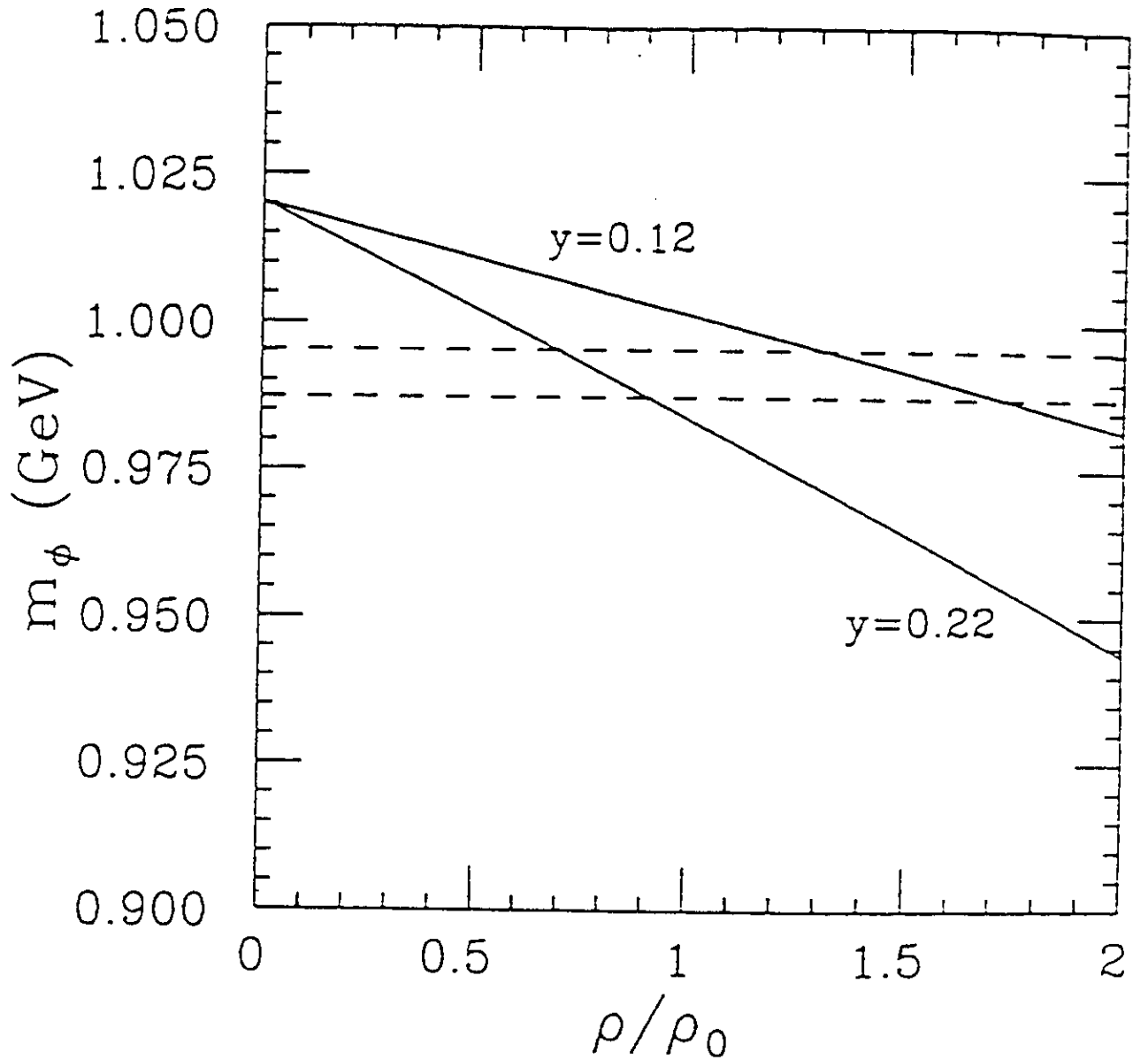


Fig.9.

ϕ -meson mass with two typical values of y (the strangeness content in the nucleon). Dashed lines indicate the K^0K^0 and K^+K^- threshold at $\rho=0$ which are the main decay modes of ϕ .

S - mid-Sector plane projection and Front view

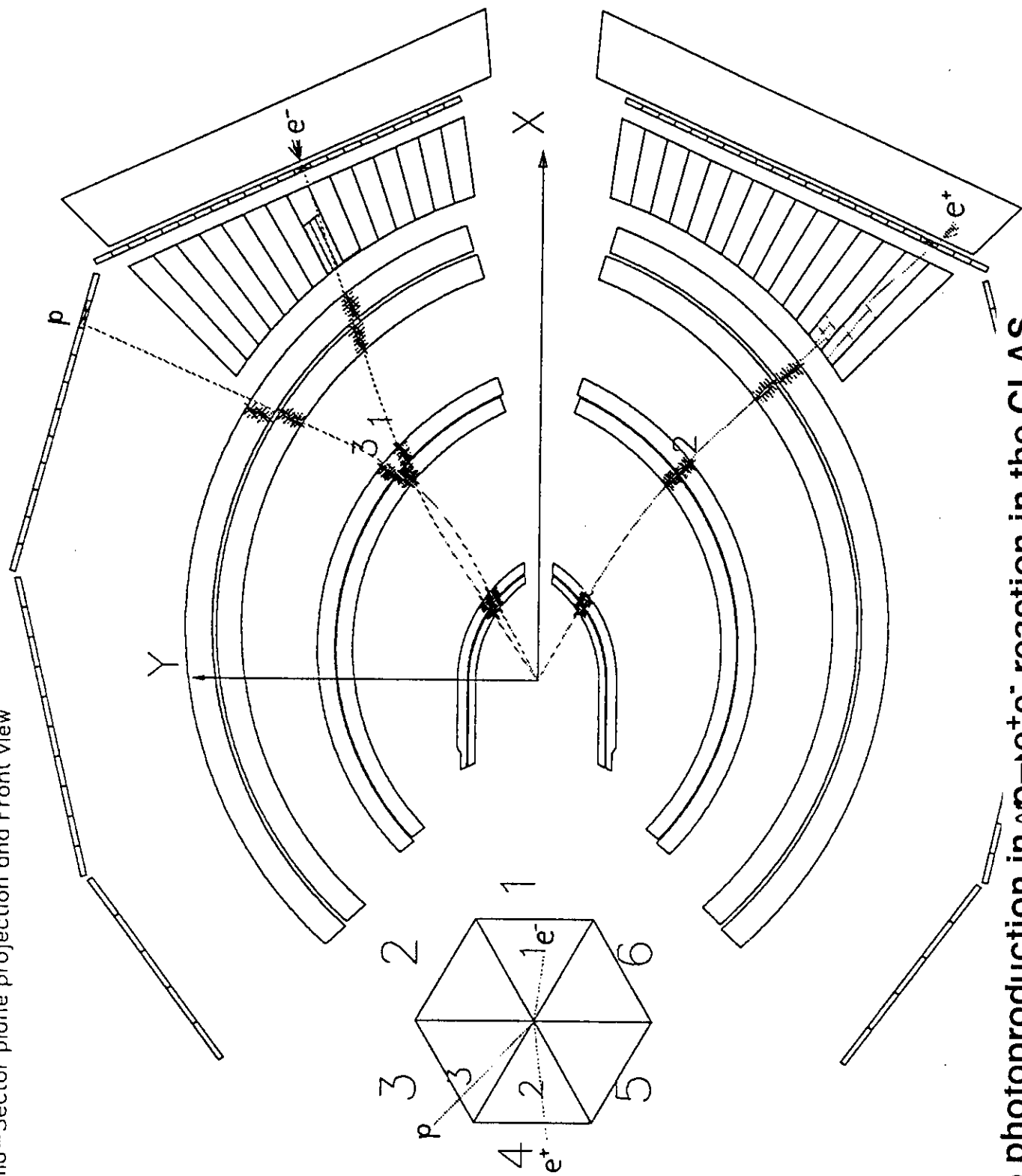


Fig.10. ω photoproduction in $\gamma p \rightarrow e^+ e^-$ reaction in the CLAS detector (sector 3 is superimposed on sector 1).

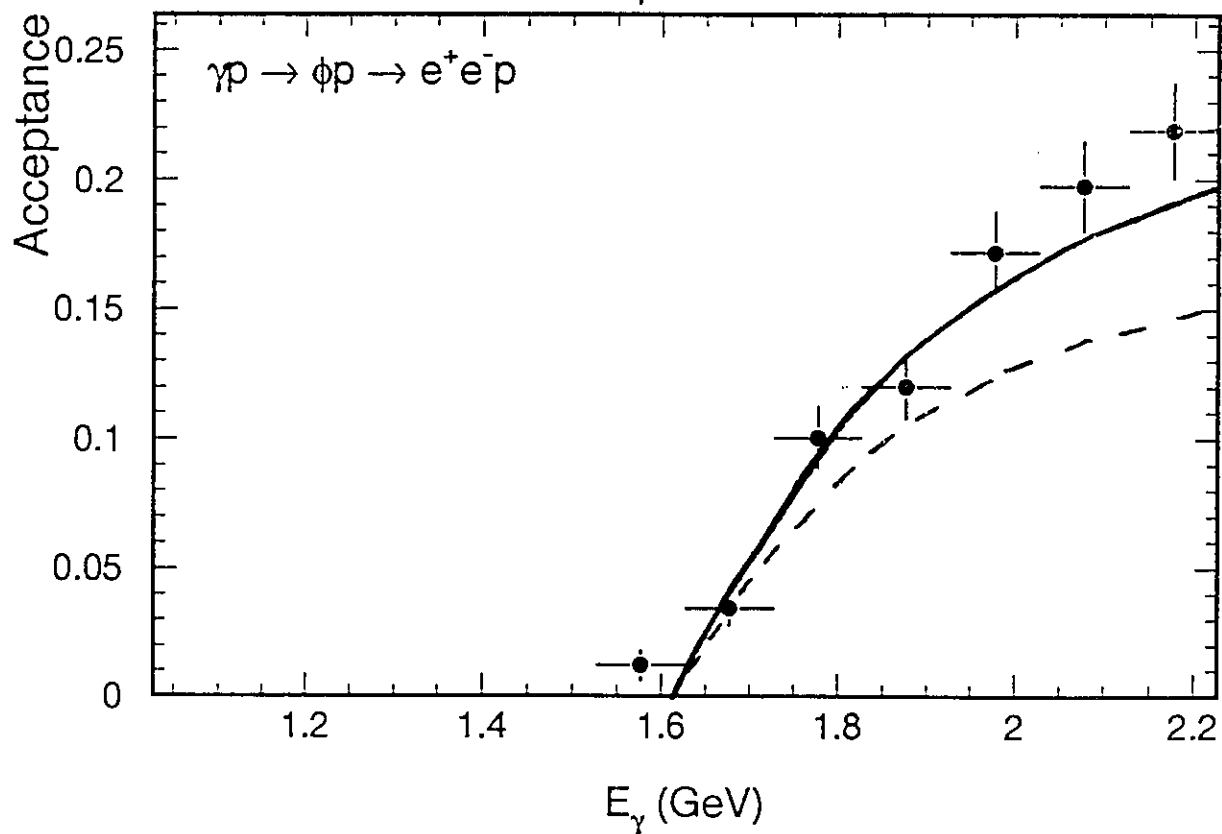
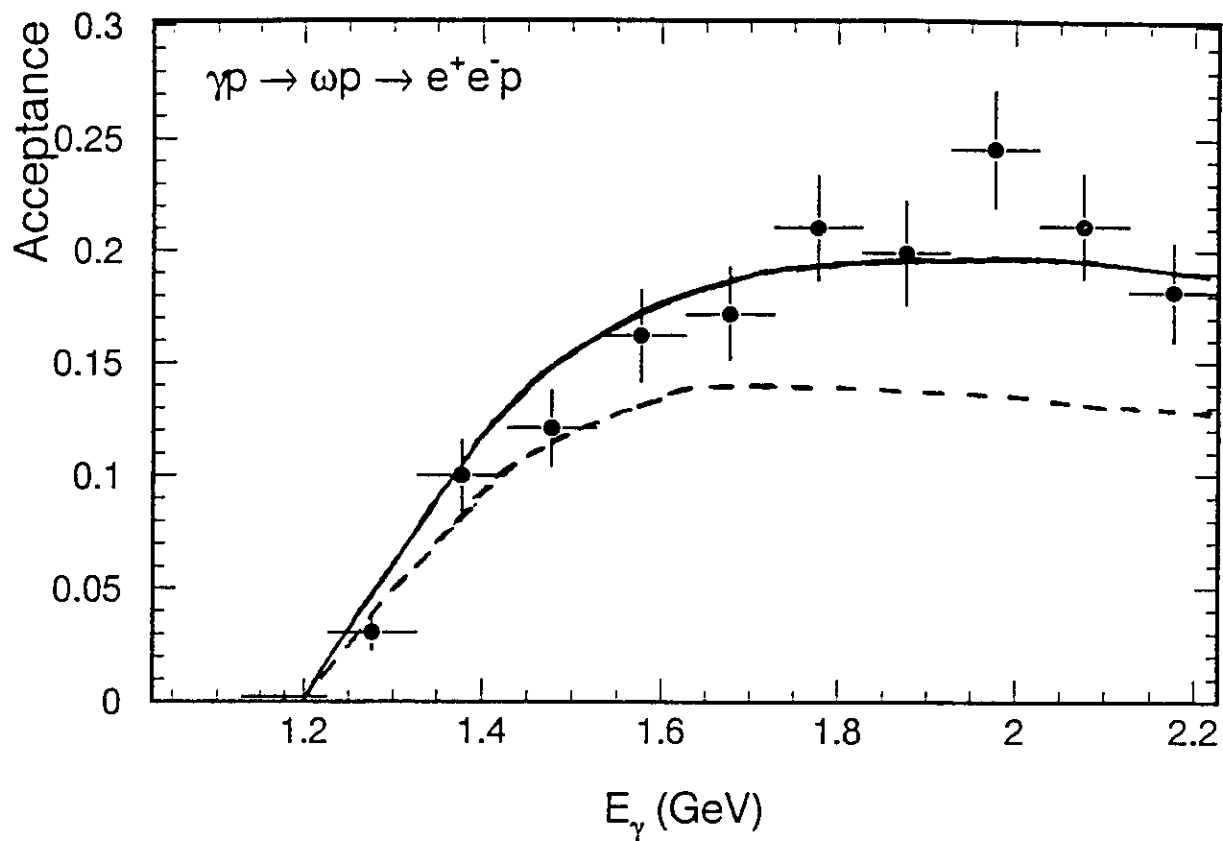


Fig.11. Acceptance calculation for ω and ϕ photoproduction.

Table 2. Count rates for vector meson photoproduction off nuclei.

Nuclide	$\rho(\text{in/out}), \text{per hour}$	$\omega(\text{in/out}), \text{per hour}$	$\phi(\text{in/out}), \text{per hour}$
^{12}C	13/7	0.7/9.3	0.5/14.5
^{56}Fe	17/3	1.0/9.0	0.7/14.3
^{207}Pb	19/1	1.5/8.5	1.0/14.0

The event rates in the CLAS detector are given in Table 2 for mesons decaying inside (in) and outside (out) of the target nucleus. It should be noted that the shift in the effective mass of the ϕ -meson is unlikely to lead to a narrow secondary peak. Since the nuclear density varies over the nuclear volume the mass shift will be smeared out.

4. Run Time Request.

We request 12 days (288 hours) of run time for the CLAS detector with a tagged photon beam intensity of $5 \cdot 10^7$ photons per second. All targets (D, C, Fe, Pb) will be in the beam and will be measured simultaneously. Vertex reconstruction will be used to distinguish the different targets. The estimated z -resolution for e^+e^- events is 0.5 mm. We propose to separate the nuclear targets by 1.4 cm and distribute the heavy targets over 2 cm intervals (Fig. 12). Distributing the targets will reduce the effects of multiple scattering of the outgoing electrons and suppress accidental coincidences by adding a vertex constraint to the time coincidence. The nuclear targets (3 cm diameter each) will be placed inside a 4 cm diameter carbon fiber tube.

We do not plan on using the start counters which will be required for the standard tagged photon beam measurements. For $\beta = 1$ particles, the start time can be reconstructed using the TOF counters of the CLAS detector. The removal of the start counters will make it feasible to use the Mini-Torus magnet (Fig. 12) to suppress the background of soft electrons which are copiously produced in heavy nuclear targets.

5. Expected results.

The expected results for 288 hours of run time are presented in Fig. 5. The error bars on the data points illustrate the expected accuracy of the proposed measurements. There are no theoretical calculations for heavy nuclei, but the accuracy of the measurements will be approximately the same. The experimental mass resolution for ω and ϕ are 4.4 ± 0.3 MeV and 6.0 ± 0.5 MeV. Note that the mass resolution of the CLAS detector is approximately an order of magnitude smaller than the predicted mass shift.

For heavy nuclear targets, the probability of bremsstrahlung emission is quite substantial (the 1 g/cm^2 Fe target is 7% in radiation length, the Pb target is 16%

in radiation length). If the bremsstrahlung photon is not detected in the CLAS electromagnetic calorimeter, bremsstrahlung emission can smear out the effective mass resolution for heavy nuclei. So special attention should be paid to the detection of additional low energy photons in the e^+e^- events (in the direction of e^+ and e^-).

6. Future Developments.

The future development of the vector meson photoproduction off nuclear targets depends on the availability of higher energy and higher intensity photon beams. At $E_o = 6$ GeV, one can investigate the photoproduction of radially excited vector mesons, e.g. $\omega'(1390)$, $\rho'(1450)$, $\omega''(1600)$, $\phi'(1680)$, and $\rho''(1700)$. If the vector meson mass shift exists, these measurements will be very interesting because all radially excited vector mesons have a short $c\tau$ (about 1 fm), and the low production cross sections are compensated by higher branching ratios for e^+e^- decays.

It is not only possible to measure the production cross sections for vector mesons but also their polarization. It is known for the photoproduction of vector mesons off hydrogen that the vector mesons are transversely polarized. The influence of the propagation of vector mesons in the nuclear medium on their polarization can be measured.

At $8 \div 12$ GeV, one can measure the production of the J/ψ -mesons near threshold. In this measurement the modification of J/ψ -meson properties in nuclear matter can be investigated. At energies $6 \div 8$ GeV one can measure the production of J/ψ -mesons below the production threshold on a free nucleon. In the proposed experiment, we will already obtain some information on the production of light quark vector mesons below threshold. On the basis of these data the feasibility of measuring J/ψ -meson photoproduction below threshold at $E_\gamma < 8$ GeV can be determined.

7. Summary.

The proposed experiment will be the first measurement of vector meson photoproduction off nuclei near threshold. The experiment is dedicated to the measurement of the vector meson mass in nuclear matter. At CEBAF energies, ρ -mesons decay mostly inside the nucleus, while ω -mesons decay mostly outside of the nucleus. ρ/ω mixing in nuclear targets (especially in the e^+e^- decay mode) can be very sensitive to the mass shift of vector mesons in nuclear matter. The mass shift has been calculated in the framework of different quark models. However, the effect has never been tested experimentally. This test is a perfect match for CEBAF because the measurements are best performed near the vector meson photoproduction threshold.

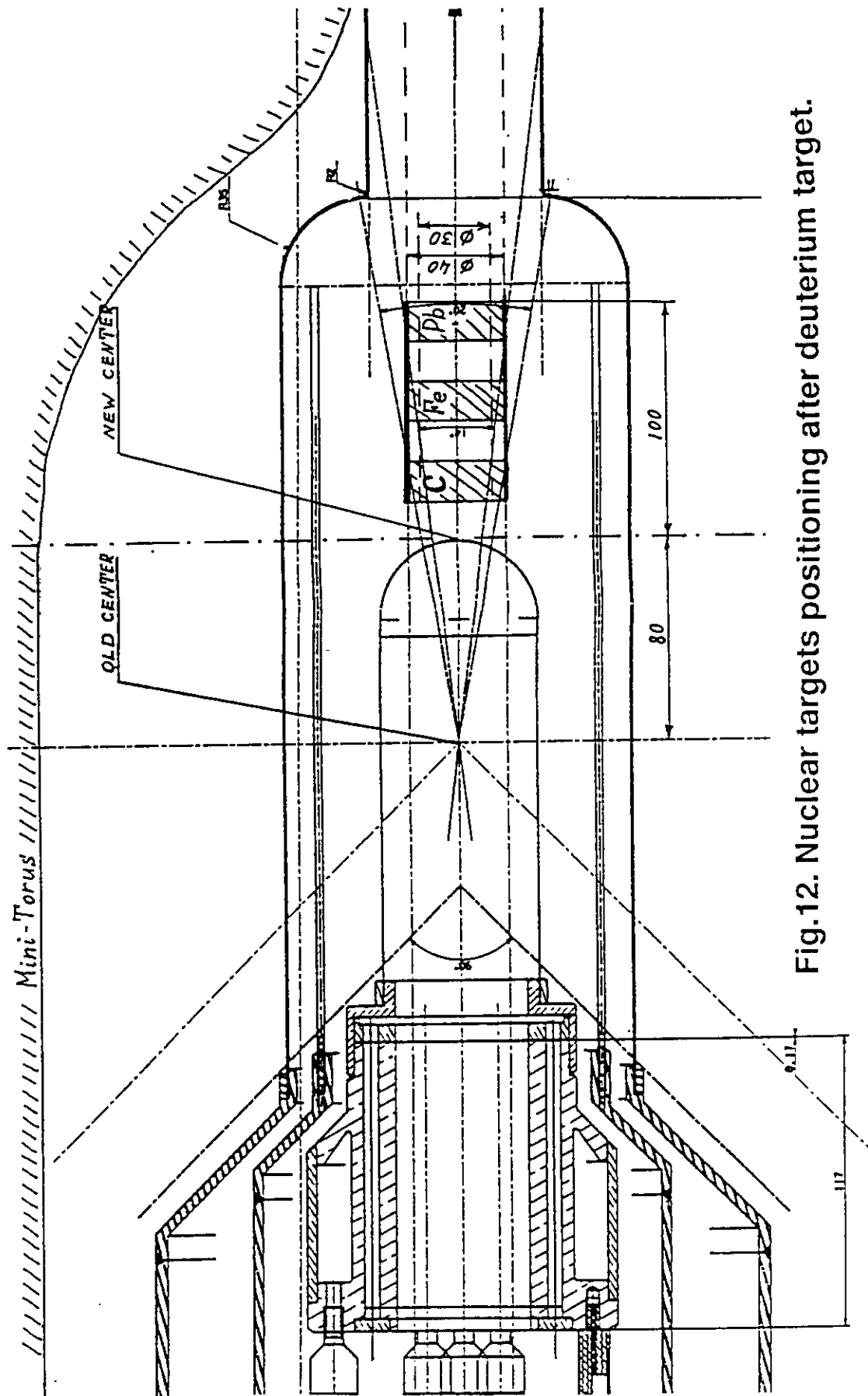


Fig.12. Nuclear targets positioning after deuterium target.

References

- 1) G.E. Brown and M. Rho, Phys. Rev. Lett. **66** (1991) 2720.
- 2) N. Isgur, Private communication.
T.D. Cohen, R.J. Furnstahl, and D.K. Griegel, Phys. Rev. Lett. **66** (1991) 961.
E.G. Drukaev and E.M. Levin, Nucl. Phys. **A511** (1990) 679.
- 3) P.Y. Bertin and P.A.M. Guichon, Phys. Rev. **C42** (1990) 1133.
- 4) P.A.M. Guichon, Phys. Lett. **B200** (1988) 235.
P.A.M. Guichon, Nucl. Phys. **A497** (1989) 265c.
- 5) T.D. Cohen, R.J. Furnstahl, and D.K. Griegel, Phys. Rev. **C45** (1992) 1881.
- 6) Y. Nambu and G. Jona-Lasinio, Phys. Rev. **122** (1961) 345; **124** (1961) 246.
- 7) M. Gell-Mann and M. Levy, Nuovo Cimento **16** (1960) 705.
- 8) P. Bicudo, Phys. Rev. Lett, **72** (1994) 1600.
- 9) M. Soyeur, Preprint LNS/Ph/93/24
B. Friman and M. Soyeur, be published
- 10) G.E. Brown et al., Phys. Rev. Lett. **60** (1988) 2723.
- 11) D. Marlow et al., Phys. Rev. **C25** (1982) 2619.
- 12) P.G. Biggs et al., Phys. Rev. Lett., **24** (1970) 1197; **24** (1970) 1201.
H. Alvensleben et al., Phys. Rev. Lett., **25** (1970) 1373; **27** (1971) 888.
- 13) J.G. Asbury et al., Phys. Rev. Lett. **19** (1967) 865; **20** (1968) 1134(E).
- 14) H. Alvensleben et al., Nucl. Phys. **B25** (1971) 333.
- 15) T. Hatsuda and Su H. Lee, Phys. Rev. **C46** (1992) R34.
- 16) H. Fraas and D. Schildknecht, Nucl. Phys. **14** (1969) 543.
- 17) H. Fraas, Nucl. Phys. **B36** (1972) 191.
- 18) P. Joos et al., Nucl. Phys. **B113** (1976) 53; **B122** (1977) 365.